Evaluation of soil-concrete interface
shear strength based on LS-SVM

Chunshun Zhang [1,3a], Jian Ji [*2,3], Yilin Gui [4],
Jayantha Kodikara [3], Sheng-Qi Yang [1] and Lei He [5]

[1] *State Key Lab for Geomechanics and Deep Underground Engineering,
China University of Mining and Technology, Xuzhou, P.R. China*
[2] *Key Lab of Ministry of Education for Geomechanics and Embankment Engineering,
Hohai University, Nanjing, P.R. China*
[3] *Department of Civil Engineering, Monash University, Australia*
[4] *School of Civil and Environmental Engineering, Nanyang Technological University, Singapore*
[5] *School of Civil Engineering, Southeast University, Nanjing, P.R. China*

Abstract. The soil-concrete interface shear strength, although has been extensively studied, is still difficult to predict as a result of the dependence on many factors such as normal stresses, surface roughness, particle sizes, moisture contents, dilation angles of soils, etc. In this study, a well-known rigorous statistical learning approach, namely the least squares support vector machine (LS-SVM) realized in a ubiquitous spreadsheet platform is firstly used in estimating the soil-structure interface shear strength. Instead of studying the complicated mechanism, LS-SVM enables to explore the possible link between the fundamental factors and the interface shear strengths, via a sophisticated statistic approach. As a preliminary investigation, the authors study the expansive soils that are found extensively in most countries. To reduce the complexity, three major influential factors, e.g., initial moisture contents, initial dry densities and normal stresses of soils are taken into account in developing the LS-SVM models for the soil-concrete interface shear strengths. The predicted results by LS-SVM show reasonably good agreement with experimental data from direct shear tests.

Keywords: soil-concrete interface shear strength; modified direct shear test; LS-SVM; statistical prediction

1. Introduction

The shear strength of soil-structure interface which determines the interface skin resistance is an important parameter in design of deep and shallow foundations, and retaining walls. In practice, most practitioners simply consider the interface shear strength as an empirical ratio to the contacted soil strength. The empirical ratios are generally determined from a series of shear tests using direct shear apparatus (Potyondy 1961, Acar *et al.* 1982, Jewell and Wroth 1987, O'Rourke *et al.* 1990, Chu and Yin 2006, Cabalar 2016, Aksoy *et al.* 2016), simple shear apparatus (Shakir and Zhu 2009), torsional shear devices (Evans and Fennick 1995), and/or ring shear devices

---

*Corresponding author, Ph.D., E-mail: jian.ji@monash.edu
[a] Ph.D., Research Fellow, E-mail: ivan.zhang@monash.edu

(Yoshimi and Kishida 1981). A general finding from these experimental studies shows that the mechanism of the interface shear strength is very complicated, associating with normal stresses, surface roughness, contacted soil densities, particle sizes, moisture contents, and dilation angle of the soils (Mitchell and Soga 1976, Kanji and Wolle 1977, Lupini *et al.* 1981, Acar *et al.* 1982, Jewell and Wroth 1987, Uesugi *et al.* 1990, Hu and Pu 2004, Chu and Yin 2006, Joseph 2012, Wang *et al.* 2013).

As a result of relevant tests, various forms of empirical relationship between interface shear strength and soil properties have been proposed, considering various infuential factors (Potyondy 1961, Kulhawy and Peterson 1979, Williams and Houlihan 1987, O'Rourke *et al.* 1990, Hossain and Yin 2013). For example, Potyondy (1961) proposed the ratio of designed frictional resistance of construction materials is from 0.4 for saturated loose sand to 1.0 for saturated dense sand. More recently, Hossain and Yin (2013) considered the grout pressure as an additional factor that enhances the soil-cement interface strength and proposed a new equation to predict the interface shear stress at failure. However, a broadly accepted and applicable method to determine the interface shear strength is yet to achieve, perhaps due to shear transfer mechanism is too complicated. As a result, a simple closed-form solution to properly define such a complex behavior may not be practical.

Given the above considerations, this paper attempts to revisit the issue from a different perspective in statistical point of view. As a preliminary analysis, a series of direct shear tests of soil-concrete interface were carried out by varying three fundamental parameters, e.g., applied normal stress σ_N, initial moisture content *w*, and initial dry density γ_d. Two types of interface shear strength, namely, the peak shear strength and the shear strength at steady state of the test, are respectively investigated. Note that with regard to the post-peak shear strength of the soil-concrete interface subjected to large displacement, the residual shear strength is used in this paper in lieu of the well-known steady-state shear strength, which is deemed appropriate as seen in the literature (Joseph and Graham-Eagle 2015). From the shear test, high nonlinear relationships between the interface shear strengths and these fundamental parameters are observed. To better understand their physical interrelationships, the statistical machine learning approaches such as Gaussian process (Kang *et al.* 2015), multivariate adaptive regression splines (Zhang and Goh 2013), support vector machines (Ji *et al.* 2015), etc., are deemed to be useful. In this study, least squares support vector machine (LS-SVM) models are developed to estimate the interface shear strengths in unknown conditions. A reasonably good prediction of the interface shear strengths is attained for new tested soil samples. This statistical learning approach may bypass the complicated analysis of soil-structure interaction mechanism, and only relies on a certain number of results from shear tests that are relatively simple and straightforward to conduct.

2. Test method for soil-concrete interface shear strength

2.1 Soil samples

The global extent of unsaturated expansive soils is very large, particularly in tropical areas. In this paper, a typical unsaturated soil in China's Nanning Province, Nanning expansive soil, was used in the direct shear tests. Expansive soils are generally grey-white alluvial or diluvial soils mainly made of highly active clay minerals such as montmorillonite, kaolinite, and illite. Expansive soils are known to produce substantial volume change due to variation in moisture

Table 1 Basic physical properties of Nanning expansive soil

Type of soil	Liquid limit /%	Plastic limit /%	Plasticity index /%	Optimum moisture content /%	Dry density limit /g·cm^{-3}	Free expansive ratio /%
Nanning expansive soil	61.4	22.8	38.6	15.8	1.89	62.5

contents. Nevertheless, the expansivity of the soil has not been included in the current investigation.

The fundamental properties of the expansive soil studied in this paper are listed in Table 1. According to Standard-IS-1498 (1970), the soil can be defined as high to very high degree of expansion considering its high liquid limit and plasticity. However, many other soil classification schemes such as the MIT particle size classification and Casagrande Unified Soil Classification System (USCS) (Howard 1977), and the American Association of State Highway and Transportation Officials Method (AASHTO 1998), have not provided assessment of the soil expansivity.

A total of 67 soil samples have been prepared. These test samples vary in moisture content, dry density and normal stress. There are four different initial moisture contents, i.e., 14.1%, 15.8%, 17.8%, and 20.8%, four different initial dry densities, i.e., 1.61g/cm^3, 1.67g/cm^3, 1.71g/cm^3, 1.76 g/cm^3 and 1.80 g/cm^3, and four different normal stresses, i.e., 25 kPa, 50 kPa, 75 kPa and 100 kPa. All soil samples were prudently prepared in compliance with the Standard Test Methods of Soils (The Ministry of Water Resources 1999). The detailed steps are briefly described as follows:

(1) Sieve the grinded air-dried soil with 2 mm meshes and measure the initial moisture content of the sieved soil;

(2) Add sufficient water to reach the required moisture content and well mix the soil, store the mixed soil in a plastic bag and seal off the bag, and then put the soil bag in a jar with a good seal for 24 hours to let the water distribute evenly;

(3) After 24 hours, get a small amount of the soil oven dried at temperature of 105°C to 110°C for over 8 hours to measure the actual moisture content; based on that, add the enough mass of the soil to fit into a cutting ring to achieve the required dry density;

(4) Place two cutting rings back-to-back on an even table surface, pour the soil sample into the cutting rings, and gently strike a ring-sized cylindrical metallic block in the upper ring by using a light hammer till the block just fits the whole volume of the upper ring.

2.2 Test apparatus

As illustrated in Fig. 1, the direct shear device was modified by putting an appropriately sized concrete block in the lower shear box. The top surfaces of the concrete block and the lower shear box were at the same level. The standard soil samples with 61.8 mm in diameter and 20.0 mm in height were then placed on the concrete block. A porous stone was placed over the top of the soil sample to simulate the drainage condition. In the relatively simple direct testing procedure of this study, the soil samples were pre-compacted before contacting with the concrete base and a thickness of interface zone was not considered, therefore the studied interface may be considered as a precast interface as explained in Hossain and Yin (2013).

The device was controlled by a constant speed of shearing at 0.02 mm/min under four normal
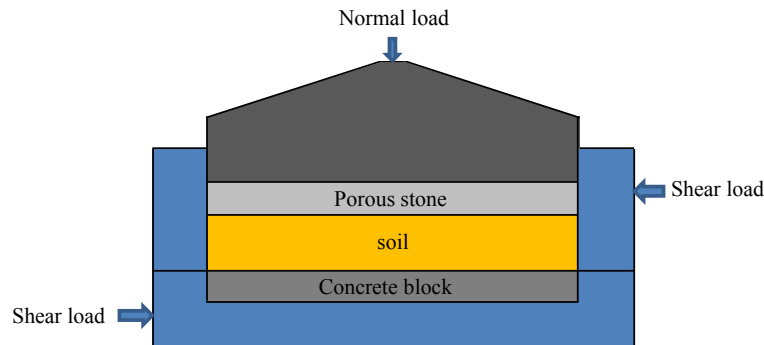
Fig. 1 Schematic of modified direct shear device

stresses of 25 kPa, 50 kPa, 75 kPa and 100 kPa, respectively. The data of shear stresses and relative shear displacements were automatically collected by a data collection system (TSW-3 model, produced by Nanjing Electric Power Automation Equipment Factory Ministry of Energy, P.R. China). Ceased the testing when shear stress remains approximately unchanged or the shear displacement was up to 4 mm.

3. Experimental results

By varying the initial soil moisture content w, initial dry density γ_d, and the applied normal stress, experimental results of peak and residual shear strengths at the soil-concrete interface are plotted, respectively, as seen in Figs. 2 and 3. Overall, both peak and residual shear strengths are proportionally increased with the normal stresses, i.e., the applied vertical loads on samples. However, significantly irregular relationships between the interface shear strengths and the two soil properties w and γ_d were clearly observed. It can be further expected if more factors are considered such as surface roughness, granular diameter, dilation angle of soils and the ways the structure is formed in, the shear strengths may tend to be more randomly distributed. Therefore it
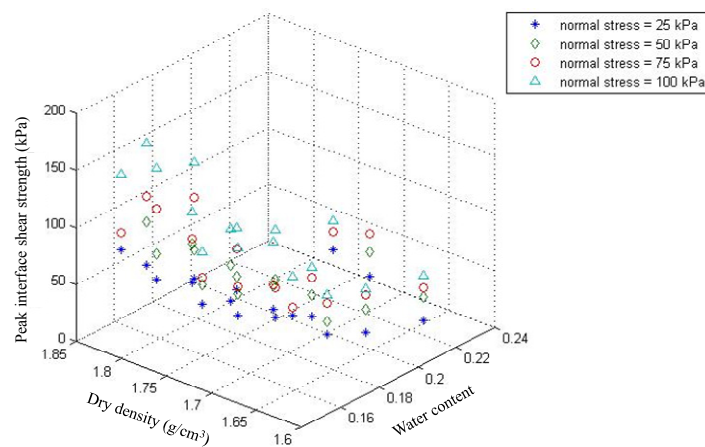

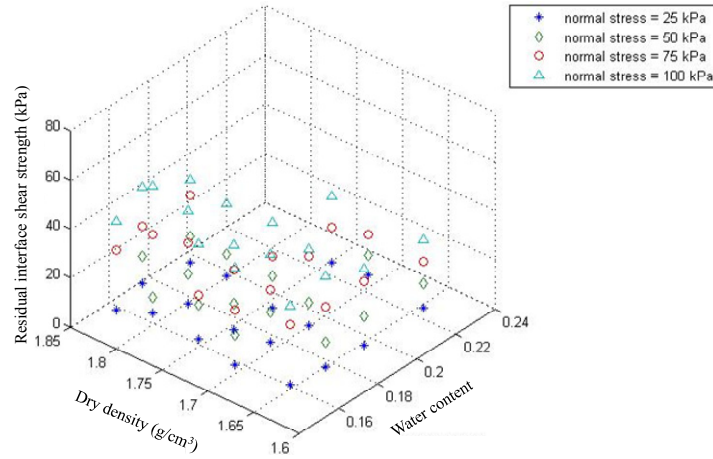Fig. 2 Scattered peak shear strength of soil-concrete interface

Fig. 3 Scattered residual shear strength of soil-concrete interface

is extremely difficult or even impossible to find a generic closed-form solution to accurately predict their inter-relationships using a common non-linear regression analysis. This problem, however, can be easily handled by data driven statistical learning models. In the following sections, a novel study on the experimental data by using the recently developed statistical learning approach, the LS-SVM, is introduced subsequently.

4. Strength estimation by LS-SVM

4.1 Basic concepts of LS-SVM

Least squares support vector machine, LS-SVM (Suykens and Vandewalle 1999, Suykens *et al*. 2002) is an alternative form of SVM which was pioneered by Vapnik and his colleagues (Vapnik 2000). Because LS-SVM provides a computational convenience over SVM by converting quadratic optimization problem into a system of linear equations, it has been attracting more and more research interests in various fields during the past decade (Zhao *et al*. 2014, Ji *et al*. 2015). To successfully implement this approach, sufficient experimental data are usually required. The data are then grouped into training and testing sets. Each instance in the training set contains one "target value" (i.e., output variable) and "several attributes" (i.e., the features or input variables). The goal of LS-SVM is to produce a surrogate model (based on the training data set) which predicts the target values of the testing data given only the testing data attributes. Formulation of LS-SVM for complex function estimation is briefly given below.

For a given training set of N data points [$\mathbf{x}_i$, y_i] ($i = 1, 2, . . ., N$) with input data $\mathbf{x}_i \ni \boldsymbol{R}^n$ and output $y_i \ni \boldsymbol{R}$, where $\boldsymbol{R}^n$ is an n-dimensional vector space and $\boldsymbol{R}$ is a one-dimensional vector space. In describing the LS-SVM for function estimation, the following optimization problem is formulated in the so-called primal weight space (Suykens *et al*. 2002)

$$\text{Minimize:} \qquad J(\mathbf{w},\mathbf{e}) = \frac{1}{2}\mathbf{w}^T\mathbf{w} + \gamma\frac{1}{2}\sum_{i=1}^{N}e_i^{\,2} \qquad (1)$$

$$\text{Subject to:} \qquad y_i = \mathbf{w}^T \varphi(\mathbf{x}_i) + b + e_i, \qquad i = 1, \ldots, N \tag{2}$$

where J is cost function consisting of fitting errors e_i, and γ is a positive real constant reflecting the relative importance of the regularization term; $\mathbf{w}$ is an adjustable weight vector in primal weight space, and $\mathbf{w} \ni R^n$; b is the bias, and $b \ni r$.

In particular, the nonlinear function $\varphi(\cdot)$ maps the basic input data $\mathbf{x}_i$ into a higher dimensional feature space. For regression analysis, it will convert the highly nonlinear target function to a linear one which helps establish a simpler cost function as shown in Eq. (1).

In primal weight space, LS-SVM model reads

$$y(\mathbf{x}) = \mathbf{w}^T \varphi(\mathbf{x}) + b \tag{3}$$

Since the weight vector $\mathbf{w}$ can be of infinitely high dimensions, it is impossible to directly calculate $\mathbf{w}$ from Eq. (1). Instead, the LS-SVM model is constructed in a so-called dual space. To do so, the Lagrangian is first defined such as

$$\mathcal{L}(\mathbf{w}, b, \mathbf{e}; \boldsymbol{\alpha}) = J(\mathbf{w}, \mathbf{e}) - \sum_{i=1}^{N} \alpha_i \{ [\mathbf{w}^T \varphi(\mathbf{x}_i) + b + e_i] - y_i \} \tag{4}$$

with Lagrange multipliers $\alpha_i \ni R$. These α_i's compose the so-called support vector $\boldsymbol{\alpha}$.

The optimality for this Lagrangian is determined by the following equation set

$$\begin{cases} \partial \mathcal{L}/\partial \mathbf{w} = 0 : & \mathbf{w} = \boldsymbol{\alpha}^T \varphi(\mathbf{x}_i) \\ \partial \mathcal{L}/\partial b = 0 : & \sum_{i=1}^{N} \alpha_i = 0 \\ \partial \mathcal{L}/\partial e_i = 0 : & \alpha_i = \gamma e_i \\ \partial \mathcal{L}/\partial \alpha_i = 0 : & \mathbf{w}^T \varphi(\mathbf{x}_i) + e_i - y_i = 0 \end{cases} \qquad i = 1, \ldots, N \tag{5}$$

The support vector $\boldsymbol{\alpha}$ and bias term b are the solutions of linear equations given by Eq. (6) (Suykens *et al*. 2002). For larger size data problem, fast solution of $\boldsymbol{\alpha}$ and b is attainable by using iterative methods such as conjugate gradient algorithm.

$$\begin{bmatrix} 0 & \mathbf{1}_v^T \\ \mathbf{1}_v & \boldsymbol{\Omega} + \frac{1}{\gamma}\mathbf{I} \end{bmatrix} \begin{Bmatrix} b \\ \boldsymbol{\alpha} \end{Bmatrix} = \begin{Bmatrix} 0 \\ \mathbf{y} \end{Bmatrix} \tag{6}$$

where column vectors $\mathbf{1}_v = [1, \ldots, 1]$, $\boldsymbol{\alpha} = [\alpha_1, \ldots, \alpha_N]$, $\mathbf{y} = [y_1, \ldots, y_N]$, and $\boldsymbol{\Omega}$ is a matrix consisting of entries $\Omega_{ij} = \varphi(\mathbf{x}_i)^T \varphi(\mathbf{x}_j)$ for $i, j = 1$ to N. The mapping function $\varphi(\cdot)$, according to Mercer's condition, can be characterized by a kernel function $K(\cdot, \cdot)$

$$K(\mathbf{x}_i, \mathbf{x}_j) = \varphi(\mathbf{x}_i)^T \varphi(\mathbf{x}_j), \qquad i, j = 1, \ldots, N \tag{7}$$

Two commonly used kernel functions are the radius basis function (RBF) $K(\mathbf{x}_i, \mathbf{x}_j) = \exp\left\{ \dfrac{-\|\mathbf{x}_i - \mathbf{x}_j\|^2}{\sigma^2} \right\}$, and the polynomial kernel $K(\mathbf{x}_i, \mathbf{x}_j) = (\mathbf{x}_i^T \mathbf{x}_j + 1)^\sigma$, where σ is a predefined constant.

As a result, the LS-SVM model for functional prediction is obtained in the form of

$$y(\mathbf{x}) = \sum_{i=1}^{N} \alpha_i K(\mathbf{x}, \mathbf{x}_i) + b \tag{8}$$

The solution of LS-SVM substantially depends on two unknown constants, i.e., kernel constant σ and the positive regularization constant γ. To find the optimal solution of LS-SVM, these constants are determined by trial and error, and a grid search method has proven to be useful (Hsu *et al*. 2010). In addition, to avoid over-training, a cross-validation technique based on a training (learning) data set and a validation data set is commonly adopted. This is somewhat similar to the cross-validation procedure required in the well-known neural network approach. However, very few model parameters are involved in the LS-SVM and there is no issue of being trapped in local minimums, hence the computational effort is much less than the neural network.

The attributes of a data set can be of different orders of magnitude, bring some numerical difficulties in the construction of LS-SVM. As a result, scaling of the data attributes is usually conducted for the computational efficiency (although not a necessity). Three methods are usually well known for rescaling data: min-max normalization, standardization (Gaussian normalization) and sigmoid normalization. In this study, the standardization technique is used for data scaling.

4.2 Soil-concrete interface shear strength predictions based on LS-SVM

Based on the experimental data as depicted in Section 3, this paper uses LS-SVM to learn the complicated interrelationships between soil-concrete interface shear resistances and the basic expansive soil properties. The input variables used for developing LS-SVM model in this study are normal stress σ_N, initial moisture content w, and initial dry density γ_d, and the target is to predict soil-concrete interface shear resistances in terms of both peak and residual shear strengths. The experimental data sets were randomly divided into training set and testing set. For the optimality
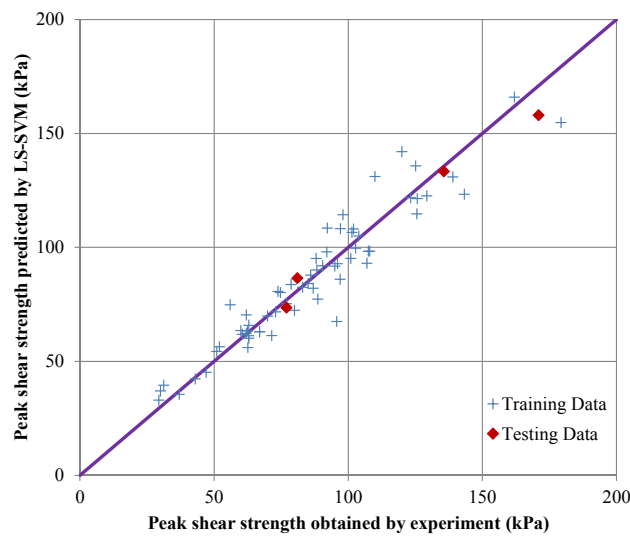

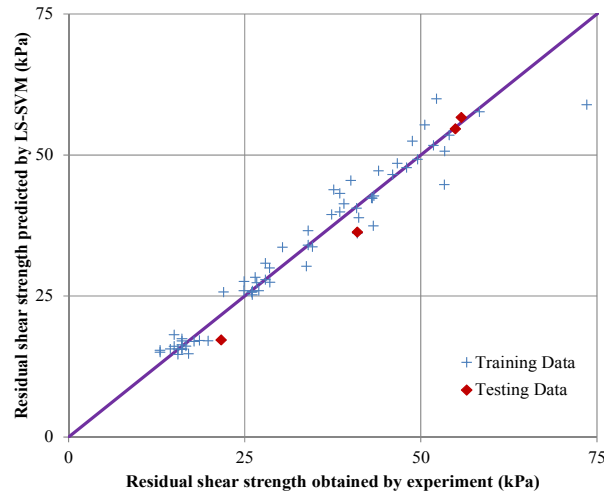Fig. 4 Peak shear strength analyzed by LS-SVM model with cross-validation

Fig. 5 Residual shear strength analyzed by LS-SVM model with cross-validation
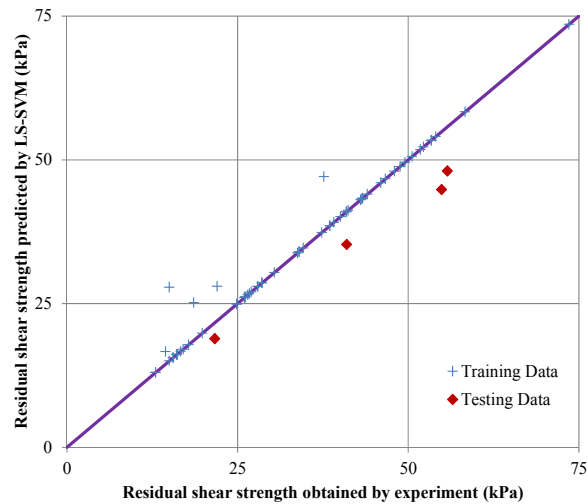

Fig. 6 Residual shear strength analyzed by LS-SVM model without cross-validation

of LS-SVM development, the grid search method with 10-fold cross-validation has been properly adopted. The numerical procedure was realized in a ubiquitous Microsoft Excel with Visual Basic

With the assistance of the present LS-SVM models, the scattered isolated experimental data of peak and residual interface shear strengths as shown in Figs. 2 and 3 can be manipulated to produce continuous and smooth envelope surfaces of shear strengths, as seen in Figs. 7 and 8. It is worth pointing out that the envelope surfaces are capable to capture most of the measured scattered shear strengths, which is the natural consequence of the good fittings as shown in Figs. 4 and 5.

From the envelop surfaces, it is anticipated that the higher the normal stress, the higher the peak and residual interface shear strengths would be. Abu-Farsakh *et al.* (2007) reported that the peak interface shear strength tends to be linearly increased with the normal stress applied, in particularly when the test samples are performed at their maximum dry density and/or optimum moisture
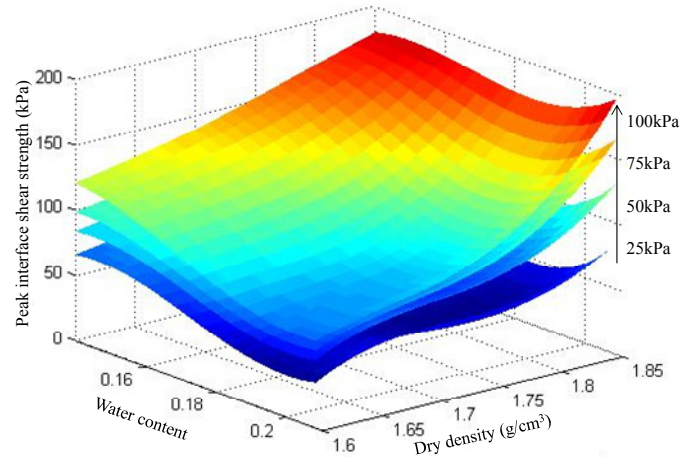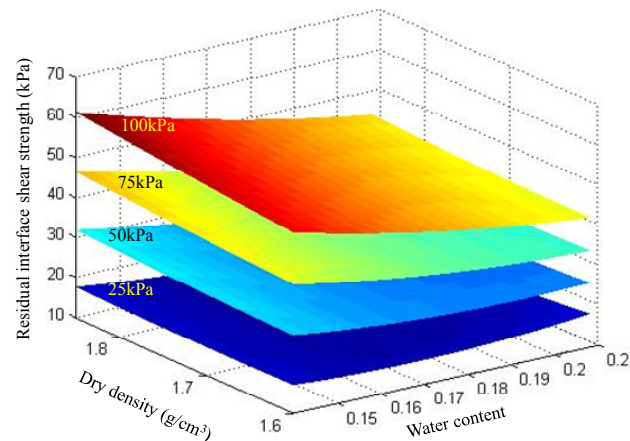
Fig. 7 Peak shear strength envelops from LS-SVM result

Fig. 8 Residual shear strength envelops from LS-SVM result

content. Nevertheless, they did not reflect the complexity of the impact of varied moisture contents on the interface shear strength under different normal stresses. In this study, it is found both from experiments and statistical learning models that the peak strength envelopes appear to be highly nonlinearly related to w, γ_d and σ_N, as shown in Fig. 7. The nonlinearity appears to be more significant at low σ_N of 25 kPa and 50 kPa than the relatively high σ_N of 75 kPa and 100 kPa. This may be contributed by soil dilation that changes with the variation in γ_d and σ_N. In addition, the nonlinearity of peak interface shear strength also tends to reduce with the decrease of initial water content.

In contrast, Fig. 8 shows that the residual interface shear strength appears to be an approximately linear relationship with w, γ_d and σ_N. As such, it suggests that unlike the highly nonlinear peak interface shear strength, the residual interface shear strength may be well predicted by a linear function formulated by the w, γ_d and σ_N, in the form of, e.g. a curved Mohr-Coulomb envelope and a critical state line, plus saturation ratio, see for example the interface strength

models discussed by Randolph *et al*. (2012). In this case, although the LS-SVM renders itself a useful tool for systematic analysis of the shear behavior, a direct algebraic link between the residual interface shear strength and the influential parameters is achievable.

Interestingly, both plots of the peak and residual interface shear strength envelopes show that under a constant normal stress σ_N, large interface shear strengths of expansive soils may be obtained when water content is low and dry density is large. On the other hand, it seems that the peak interface shear strength is more susceptible to the change of dry density while the residual interface shear strength is more to the change of water content. While these findings are solely based on the limit test results on hand, further investigation is needed to draw a more general conclusion on the influence of soil properties on soil-concrete interface shear strengths.

5. Conclusions

Through a series of direct shear tests of soil-concrete interface conducted at different w, γ_d and σ_N, this paper investigated the variations of interface shear strengths (both peak and residual) using a statistical learning approach, LS-SVM. The following conclusions can be drawn based on the discussions in this study:

(1) A well-trained LS-SVM model is capable to capture the complex relationship between the shear strength of the soil-concrete interface and some of the important soil properties. In this way, a straightforward and accurate prediction of the interface shear strength is attainable when a certain number of test results are available. This new perspective of assessing the interface shear strength can simplify the systematic considerations of the interrelationships among many physical parameters.

(2) Due to the high nonlinearity of interface shear strength, overfitting of the LS-SVM model may exist if cross-validation is not considered. For a better prediction of unknown scenarios, a simple grid search based cross-validation procedure is suggested.

(3) The modelled interface shear envelops clearly indicate that the higher the normal stress, the higher the peak and residual interface shear strengths. The peak interface shear strength shows higher non-linearity than the residual interface shear strength, with respect to the three parameters investigated. Moreover, it is observed that the non-linearity of peak interface shear strength tends to reduce with the decrease of both normal stress and initial water content.

(4) This study provides a preliminary investigation of the soil-concrete interface shear strengths utilizing LS-SVM by considering only three fundamental influential factors, e.g., the initial water content, initial dry density and applied normal stress. Further study can be carried out to develop a more generalized LS-SVM model to account for more influential factors (e.g., surface roughness, particle sizes, dilation angle of the soils, etc) that may change the interface shear strengths.

Acknowledgments

References

AASHTO (1998), Standard Specification for Highway Bridges. American Association of State Highway and Transportation Officials; Washington, D.C., USA.

Abu-Farsakh, M., Coronel, J. and Tao, M. (2007), "Effect of soil moisture content and dry density on cohesive soil–geosynthetic interactions using large direct shear tests", *J. Mater. Civil Eng.*, **19**(7), 540-549.

Acar, Y.B., Durgunoglu, H.T. and Tumay, M.T. (1982), "Interface properties of sand", *J. Geotech. Geoenviron. Eng.*, **108**(GT4).

Aksoy, H.S., Gör, M. and İnal, E. (2016), "A new design chart for estimating friction angle between soil and pile materials", *Geomech. Eng., Int. J.*, **10**(3), 315-324.

Cabalar, A.F. (2016), "Cyclic behavior of various sands and structural materials interfaces", *Geomech. Eng., Int. J.*, **10**(1), 1-19.

Chu, L.-M. and Yin, J. (2006), "Study on soil–cement grout interface shear strength of soil nailing by direct shear box testing method", *Geomech. Geoeng.: Int. J.*, **1**(4), 259-273.

Evans, M. and Fennick, T. (1995), "Geosynthetic/soil interface friction angles using a rotation shear device", *ASTM Geotech. Test. J.*, **18**(2), 271-275.

Hossain, M.A. and Yin, J.-H. (2013), "Behavior of a pressure-grouted soil-cement interface in direct shear tests", *Int. J. Geomech.*, **14**(1), 101-109.

Howard, A.K. (1977), Laboratory Classification of Soils: Unified Soil Classification System; US Department of the Interior, Bureau of Reclamation, Engineering and Research Center, Division of Research, Geotechnical Branch.

Hsu, C.-W., Chang, C.-C. and Lin, C.-J. (2010), A Practical Guide to Support Vector Classication, Department of Computer Science, National Taiwan University.

Hu, L. and Pu, J. (2004), "Testing and modeling of soil-structure interface", *J. Geotech. Geoenviron. Eng.*, **130**(8), 851-860.

Jewell, R. and Wroth, C. (1987), "Direct shear tests on reinforced sand", *Geotechnique*, **37**(1), 53-68.

Ji, J., Zhang, C.S., Kodikara, J. and Yang, S.-Q. (2015), "Prediction of stress concentration factor of corrosion pits on buried pipes by least squares support vector machine", *Eng. Fail. Anal.*, **55**, 131-138.

Joseph, P.G. (2012), "Physical basis and validation of a constitutive model for soil shear derived from microstructural changes", *Int. J. Geomech.*, **13**(4), 365-383.

Joseph, P.G. and Graham-Eagle, J. (2015), "Analytical solution of a dynamical systems soil model", *Analytical Methods in Petroleum Upstream Applications*; Computer Methods and Recent Advances in Geomechanics, pp. 219-224.

Kang, F., Han, S., Salgado, R. and Li, J. (2015), "System probabilistic stability analysis of soil slopes using Gaussian process regression with Latin hypercube sampling", *Comput. Geotech.*, **63**, 13-25.

Kanji, M. and Wolle, C. (1977), "Residual strength new testing and microstructure", *Proceedings of the 9th ICSMFE*, Tokyo, Japan, July, Volume 1, pp. 153-154.

Kulhawy, F. and Peterson, M. (1979), "Behavior of sand-concrete interfaces", *Proceedings of the 6th Panamerican Conference on Soil Mechanics and Geotechnical Engineering*, Lima, Peru, September.

Lupini, J., Skinner, A. and Vaughan, P. (1981), "The drained residual strength of cohesive soils", *Geotechnique*, **31**(2), 181-213.

Mitchell, J.K. and Soga, K. (1976), *Fundamentals of Soil Behavior*, Wiley, New York, NY, USA.

O'Rourke, T., Druschel, S. and Netravali, A. (1990), "Shear strength characteristics of sand-polymer interfaces", *J. Geotech. Eng.*, **116**(3), 451-469.

Potyondy, J.G. (1961), "Skin friction between various soils and construction materials", *Geotechnique*, **11**(4), 339-353.

Randolph, M., White, D. and Yan, Y. (2012), "Modelling the axial soil resistance on deep-water pipelines", *Géotechnique*, **62**(9), 837-846.

Shakir, R. and Zhu, J. (2009), "Behavior of compacted clay-concrete interface", *Frontiers of Architecture and Civil Engineering in China*, **3**(1), 85-92.

Standard-IS-1498 (1970), Classification and Identification of Soils for General Engineering Purposes; New

Delhi, India.

Suykens, J.A.K. and Vandewalle, J. (1999), "Least squares support vector machine classifiers", *Neural Processing Lett.*, **9**(3), 293-300.

Suykens, J.A.K., De Brabanter, J., Lukas, L. and Vandewalle, J. (2002), "Weighted least squares support vector machines: robustness and sparse approximation", *Neurocomputing*, **48**(1-4), 85-105.

The Ministry of Water Resources, P.R.C. (1999), *Test Methods of Soils*, WaterPower Press, Beijing, China; SL237-1999.

Uesugi, M., Kishida, H. and Uchikawa, Y. (1990), "Friction between dry sand and concrete under monotonic and repeated loading", *Soils Found.*, **30**(1), 115-128.

Vapnik, V. (2000), The nature of statistical learning theory, Springer Science & Business Media.

Wang, C.H., Jin, K. and Zhan, C. (2013), "Model test studies of the mechanical properties of pile-soil interface", *Appl. Mech. Mater.*, **392**, 904-908.

Williams, N. and Houlihan, M. (1987), "Evaluation of interface friction properties between geosynthetics and soils", *Proceedings of Geosynthetics*, **87**, 616-627.

Yoshimi, Y. and Kishida, T. (1981), "Friction between sand and metal surface", *Proceedings of the 10th International Conference on Soil Mechanics and Foundation Engineering*, Stockholm, Sweden, June.

Zhang, W.G. and Goh, A.T.C. (2013), "Multivariate adaptive regression splines for analysis of geotechnical engineering systems", *Comput. Geotech.*, **48**, 82-95.

Zhao, H., Ru, Z., Chang, X., Yin, S. and Li, S. (2014), "Reliability analysis of tunnel using least square support vector machine", *Tunn. Undergr. Space Technol.*, **41**, 14-23.

CC